GPS Solut (2006) 10: 219–228
DOI 10.1007/s10291-006-0029-5

ORIGINAL ARTICLE

William Rideout
Anthea Coster

Automated GPS processing for global total electron content data

Received: 14 October 2005
Accepted: 6 April 2006
Published online: 11 May 2006

W. Rideout · A. Coster (✉)
MIT Haystack Observatory,
Atmospheric Sciences, Off Route 40,
Westford, MA 01886, USA
E-mail: ajc@haystack.mit.edu
Tel.: +1-781-9815753
Fax: +1-781-9815766

Abstract A software package known as MIT Automated Processing of GPS (MAPGPS) has been developed to automate the processing of GPS data into global total electron density (TEC) maps. The goal of the MAPGPS software is to produce reliable TEC data automatically, although not yet in real time. Observations are used from all available GPS receivers during all geomagnetic conditions where data has been successfully collected. In this paper, the architecture of the MAPGPS software is described. Particular attention is given to the algorithms used to estimate the individual receiver biases. One of the largest sources of error in estimating TEC from GPS data is the determination of these unknown receiver biases. The MAPGPS approach to solving the receiver bias problem uses three different methods: minimum scalloping, least squares, and zero-TEC. These methods are described in detail, along with their relative performance characteristics. A brief comparison of the JPL and MAPGPS receiver biases is presented, and a possible remaining error source in the receiver bias estimation is discussed. Finally, the Madrigal database, which allows Web access to the MAPGPS TEC data and maps, is described.

Introduction

Since the mid-to-late 1990s, a variety of research groups have separately developed algorithms to process GPS data from the International GNSS Service (IGS) network and produce global maps of total electron content (TEC). Early work was done by Attila Komjathy at the University of New Brunswick, Canada (Komjathy 1997) and by Tony Mannucci and Brian Wilson at the Jet Propulsion Laboratory (Mannucci et al. 1998). A recent article by Komjathy et al. (2005) describes JPL's current technique for the automated processing of data from more than 1,000 GPS receivers into global TEC. Another group working with global TEC processing is the ionospheric working group of IGS which was established in 1998 (Feltens and Schaer 1998). Recently, the NOAA Space Environment Center has developed a new data assimilation product (Fuller-Rowell 2005) characterizing ionospheric TEC over the US. Some of the algorithms needed to process GPS data are available through the University of Texas at Austin's open source software project called the **GPS Toolkit**, or GPSTk (Renfro et al. 2005).

Prior to 2000, the ionospheric community was reluctant to use data from GPS receivers that were outside of the IGS and Continuously Operating Reference System (CORS) networks. It was assumed that TEC estimates from receivers not adhering to the strict standards of IGS and CORS would be suspect. MIT Haystack was the first group to make use of all available GPS data to produce strictly data-driven plots of TEC using no underlying models to smooth out gradients. Because of this, we were the first group to identify the plumes of storm enhanced density that form over the

U.S. during geomagnetic storms (Coster et al. 2001; Foster et al. 2002). GPS TEC maps provided by this method have now been widely disseminated throughout the atmospheric research community and have become one of the standard means to study the effects of geomagnetic storms on the ionosphere.

In this paper, we will describe the algorithms used in the software package MIT Automated Processing of GPS (MAPGPS). MAPGPS was developed at the MIT Haystack Observatory to automate the process of downloading and processing GPS data to produce global TEC maps. Currently, about 250 days of processed TEC data from 2000 to 2005 are available on-line. The data is provided as estimates of TEC in 1° by 1° bins every 5 min distributed over those locations where data is available. During the next year, we anticipate processing all of the remaining TEC data. The MAPGPS processing methods differ from those of other facilities, and it is instructive for the community to compare the various processing procedures described in the open literature. We will also discuss how to access the MIT processed TEC data, and other ancillary space weather data, from the Madrigal database, which is an open source, Web-based, distributed database system developed at MIT Haystack Observatory.

Automated processing of GPS data

An automated technique for processing GPS data from multiple receivers involves several steps. The first step in MAPGPS is a process for downloading and reading all available data in as many versions of RINEX, and other data formats, as possible. Currently, MAPGPS downloads the GPS data in daily segments. Once data are downloaded, "preliminary" line of sight TEC estimates are formed using a combination of processed L1 and L2 pseudorange and phase data. These preliminary TEC estimates represent the TEC values along the line of sight from each receiver to all satellites in view. Loss of lock in the carrier-phase observables is screened for and corrected (Blewitt 1990), and the carrier-phase data is used to smooth the pseudorange value. The next step involves determining the ground receiver and satellite biases and then removing them from the preliminary TEC estimates. Biases represent the additional delay between measured L1 and L2 GPS signals at the receiver due to both satellite and receiver hardware. To help determine these biases, a mapping function is applied to the data to convert each line of sight TEC estimate into a zenith TEC estimate. The next to last step in the automated processing involves screening all of the TEC data. Using a robust criterion, "bad" data must be flagged and removed from the data set. The "bad" data referred to here is assumed to be caused by specific issues within the internal firmware of certain individual receivers rather than by interference or multipath. This phenomenon will be described in more detail in Removal of outliers. Once the bad data is removed, the receiver biases are recalculated, and the final corrected TEC values are produced. Figure 1 shows an outline of the procedure MAPGPS follows to process the GPS data.

MAPGPS was designed with the goal of computing absolute values of TEC, along with their associated error bars, worldwide. A secondary goal was to produce a scalable algorithm, i.e., software that is able to process each day independently, without requiring any previous days' results. A final goal was to select the best mapping function to process the data. A mapping function is the multiplicative factor used to convert line of sight TEC to zenith TEC. To accomplish this last goal, a mapping figure of merit, defined as the average difference in estimated zenith TEC values for coincident measurements from different receivers, was used as the criterion for selection. Coincident measurements are defined as TEC estimates from different receivers separated by no more than 50 km in the horizontal location at the pierce point height of 450 km along the line of sight from the receiver to the satellite. The elevation angle cutoff used in this analysis was 7°. The 450 km altitude level was chosen for algorithm stability, and typically is at or above the F2 electron density peak altitude. This definition clearly weights the figure of merit to the more densely sampled areas, such as the continental USA. MAPGPS uses the following mapping function to minimize the mapping figure of merit:

$$z = \frac{1}{\sqrt{(1.0 - (F\cos(\mathrm{el}))^2)}}.$$

The adjustment parameter, F, was determined by selecting several representative quiet and storm/disturbed days for study. Satellite biases were fixed to the JPL values for the given day, and the receiver biases were estimated using the mapping function above following the steps described in MAPGPS receiver bias determination. Each day was analyzed a number of times with values of F, the fit parameter, varying from 0.80 to 0.98. Ultimately, a value of 0.95 was found to best minimize the value of the figure of merit, and it is this value that is used in the MAPGPS mapping function.

It is worth noting that several mapping functions have been defined in the literature (Komjathy 1997). The standard mapping function (Mannucci et al. 1993) has the same form as the one used by MAPGPS, if one sets the adjustment parameter, F, equal to $(1 + (h/R_E))^{-1}$, where h is the ionospheric shell height. The F value of 0.95 that was found to minimize the figure of merit corresponds to a value of h = 335 km (R.B. Langley, private communication). Typically a shell height of

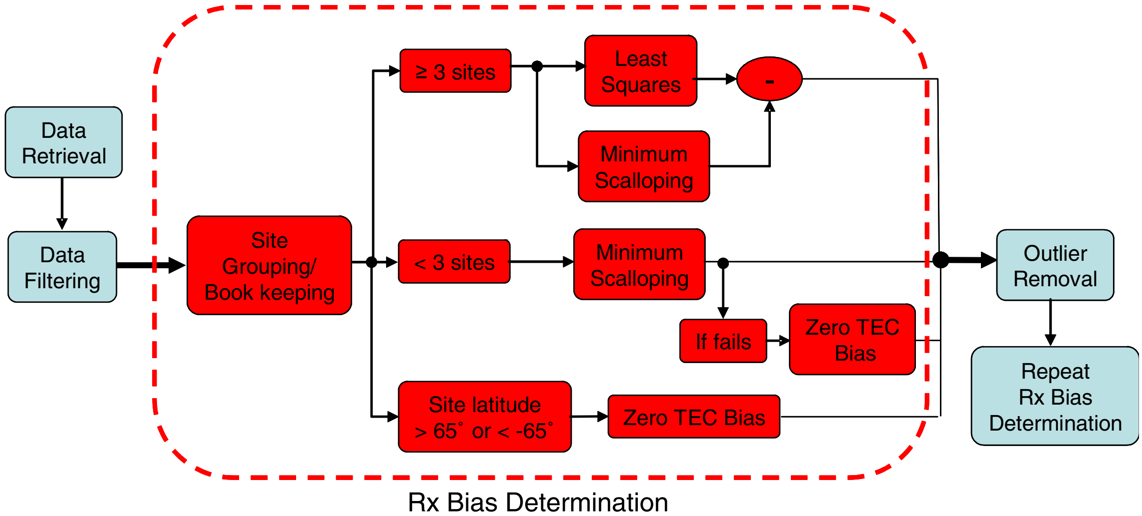

Fig. 1 Illustration of processing steps in MAPGPS

450 km is used in the determination of both the receiver and satellite biases. In fact, we used the 450 km altitude in the above definition of the figure of merit.

There are a number of possible reasons for this inconsistency. The first is that neither mapping function is entirely correct, and the strict physical interpretation of $F = (1 + (h/R_E))^{-1}$ may be in error. In addition, the F value selected in our process represents an average value over 24 h, and the ionospheric shell height varies as a function of time of day. The issue of varying scale heights has been investigated by the ionospheric research community (Komjathy and Langley 1996). Various researchers have employed a multi-shell approach for defining the mapping function with some success (Hernandez-Pajares et al. 1999; Mannucci et al. 1998). In our opinion, for the purpose of producing global TEC maps from GPS data that can be used to interpret geophysical events, any inconsistencies resulting from choosing either 335 or 450 km shell heights are not significant, but should be investigated further.

Our goal has been to provide TEC maps based entirely on GPS data with no underlying smoothing (other than averaging and use of median values). For ionospheric studies, the entire concept of a mapping function is somewhat questionable. A tomographic approach to modeling the ionosphere, based on the input of multiple data types, will eventually be able to model the ionosphere far more accurately than we are currently able to do with the limited number of GPS TEC measurements available.

Data retrieval

A python script is used to download daily RINEX files from multiple Web sites including those listed in Table 1. In addition to the GPS RINEX files, data from both the TOPEX and JASON satellites are downloaded from NASA's Crustal Dynamics Data Information System (CDDIS) site.

Determination of satellite and receiver biases

Both satellite hardware (the SV L1–L2 biases) and the receiver hardware (the receiver biases) contribute delays between the L1 and L2 signals that must be removed in order to correctly solve for the ionosphere. Ignoring these biases (which may be positive or negative) may cause errors of up to nine TEC units (TECU) for satellite biases and 30 or more TECU for receiver biases. In fact, if we examine the distribution of the 1,000 plus receiver biases that we solve for, the mean is 0.25 TECU, indicating that there is no preferential sign for the receiver bias, and the standard deviation, which is the significant statistic, is 52 TECU. (For comparison, 1 TECU is equivalent to a delay in units of distance of 0.163 m at the L1 frequency. By delay, we are referring to the ionospheric correction which would need to be made to the range measured using the L1 signal. 1 TECU is also equal to a delay in time for the L1 signal of 0.54 ns.)

These biases have been estimated by Gaposchkin and Coster (1993), Sardon et al. (1994), Wilson et al. (1999),

Table 1 List of web sites used to download GPS data

ftp://lox.ucsd.edu/pub/rinex
ftp://igs.ensg.ign.gr/pub/igs/data
ftp://garner.ucsd.edu/pub/rinex
ftp://cddis.gsfc.nasa.gov/pub/gps/data
http://www.ngs.noaa.gov/cors/rinex
http://www.naic.edu/aisr/GPSTEC/Archive/

and others. The satellite biases have been shown to be relatively constant (B.D. Wilson, private communication) and are easily available on-line. MAPGPS uses the JPL estimated values for the satellite biases which are available through CDDIS. These biases are downloaded for each day. If the current day is not available, a search is made backwards in time up to 100 days prior. If this latter condition occurs, a small amount of error is introduced in the estimation procedure. In general, the receiver bias is considerably larger than the satellite bias, and it is only very rarely that the satellite bias data is not available.

To estimate receiver biases, MAPGPS uses a procedure which relies on a combination of three different methods. The first method, minimum scalloping, was developed by P. Doherty (private communication) and depends on the assumption that the ‘‘scalloping’’ in the values of zenith TEC estimates from the different satellites observed over a 24 h period should be minimized. The second method, least squares, uses a least squares fitting routine to compute the differential receiver biases. The least squares method in MAPGPS is based on an earlier procedure developed at MIT Lincoln Laboratory (Gaposchkin and Coster 1993; K. Duh, private communication). The least squares method measures only the differential biases, however, and so must be combined with the other methods to determine absolute bias levels. The third method used by MAPGPS is the zero TEC method. Here, the bias value of the receiver is selected to be that which sets the minimum value of the TEC over a 24-h period to be zero. In the following, we describe these methods in more detail.

Minimum scalloping

The minimum scallop technique is based on the principle that zenith TEC values computed from low elevation angle data should not, on average, be different from zenith TEC values computed from high elevation angles. Of course, during some time periods, there may be temporary ionospheric structure that makes this assumption false, such as at sunset or sunrise when gradients are frequently present in the TEC. Because of this, this technique has been implemented in a way that tries to average values over a relatively long period.

In general, a mapping function converts the line-of-sight TEC at lower elevation angles to its vertical or zenith value. However, the part of the TEC observation that is caused by receiver bias, and not the ionosphere, is unaffected by elevation angle. When the mapping function is applied to a receiver using an incorrect receiver bias, the estimated vertical TEC values will be in error. Specifically, the vertical TEC values that correspond to low elevation angles will be either increased or decreased, depending on the sign of the bias. This phenomenon is illustrated in Fig. 2.

We apply the minimum scallop technique to TEC data around local midnight, where there should be less inhomogeneity in the TEC. For a given receiver bias, we bin and median filter vertical TEC values by elevation angle, and determine the flatness of the resulting median TEC versus elevation-angle plot. The receiver bias that gives the flattest value of TEC versus elevation angle is the minimum scallop receiver bias. While we have found no systematic errors associated with this technique, the

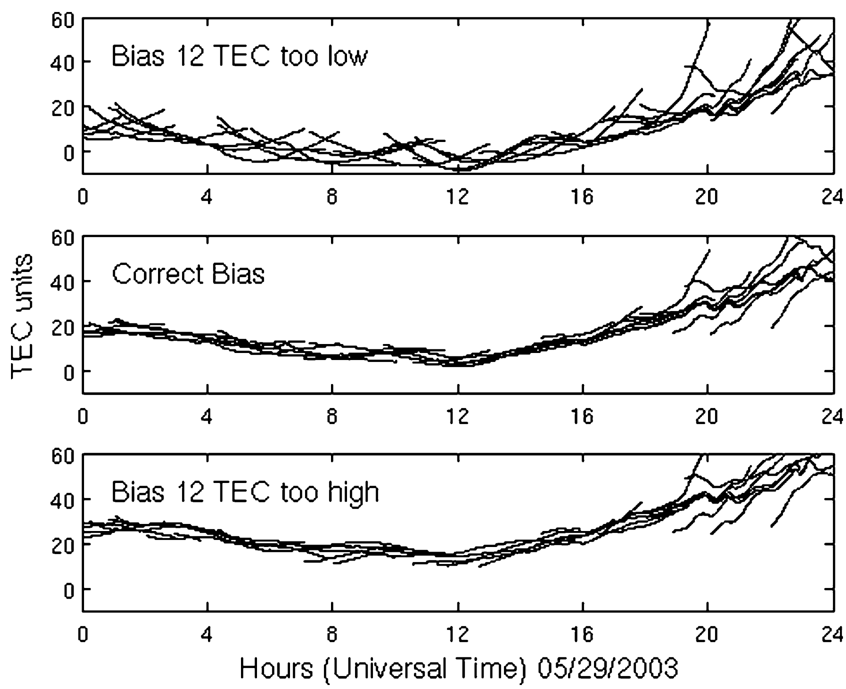

Fig. 2 Illustration of scalloping observed in zenith TEC estimates of several satellites from one receiver

standard deviation of day-to-day estimations of the same receiver is about 2 TECU. It is not clear whether this 2 TECU value is due to innate problems with the algorithm or with actual receiver bias variability, or some combination of both.

Least squares

To use the least squares method, a system of equations is set up using a number of observations and unknowns (Gaposchkin and Coster 1993; K. Duh, private communication). On any given day, each GPS receiver observes multiple satellites multiple times. Each observation consists of a TEC estimate, a satellite bias, and a receiver bias. The receiver bias is assumed to be constant over the day for each receiver, and the satellite bias is assumed to be constant over the day for each satellite. In our processing, we assume that the satellite biases are known (Wilson et al. 1999). At this time, no uncertainty information is used in our estimation procedure for the receiver biases. Eventually we hope to modify our procedure to include this.

The problem of estimating the receiver biases is overdetermined to a large degree as there are many more observations than unknown receiver biases. Accordingly, the method of least squares is well suited to find the best-fit solution. To compute the differential relationship between the different receiver biases, a system of difference observations is created as follows:

An observation, O, is described as (ignoring measurement error):

$$O = T + S + R,$$

where T is the line-of-sight TEC, S is the satellite bias, and R is the receiver bias. S is assumed to be known a priori from previous calculations, so it is subtracted as a constant, leaving the value Q, our partially corrected observation:

$$Q = O - S = T + R.$$

If there are two observations by different receivers, we have the equation:

$$Q_1 = Q_2 = (T_1 - T_2) + (R_1 - R_2)$$

Applying the vertical TEC mapping function, Z, we get:

$$\frac{Q_1}{Z_1} - \frac{Q_2}{Z_2} = \left(\frac{T_1}{Z_1} - \frac{T_2}{Z_2}\right) + \left(\frac{R_1}{Z_1} - \frac{R_2}{Z_2}\right) = (vT_1 - vT_2) + \left(\frac{R_1}{Z_1} - \frac{R_2}{Z_2}\right),$$

where $v\tau$ represents the vertical, or zenith, TEC.

If the ionosphere pierce points of the two observations are sufficiently close together, the zenith TECs cancel out and we are left with the desired equation:

$$\frac{Q_1}{Z_1} - \frac{Q_2}{Z_2} = \left(\frac{R_1}{Z_1} - \frac{R_2}{Z_2}\right).$$

The system of these equations that is generated here can be solved by the least squares method. MAPGPS defined the observations to be sufficiently close together if their ionospheric pierce point locations at 450 km were separated by no more than 100 km in the horizontal direction. The least squares method does not determine the absolute value of the biases. It only gives the relative biases.

Zero TEC method

This method is based on the principle that the TEC often approaches zero during the night or at high latitudes. Therefore, the receiver bias in this method is calculated by setting the minimum observed value of the TEC over a 24 h period equal to zero. This method has the advantage that it is simple to use, and in a relative sense, it is reasonably robust. Nevertheless, especially in the equatorial regions, one does not anticipate the minimum value of the TEC to be equal to zero. Also, noise can affect the estimation. Using this assumption to calculate the biases may cause non-negligible errors. For comparison, the GPS navigation message model always sets the night-time value to 5 ns ≈ 9 TECU @ L1 ≈ 1.5 m (R.B. Langley, private communication).

MAPGPS receiver bias determination

In MAPGPS, the receiver bias determination is an iterative process involving several steps. This process is illustrated inside the dashed line in Fig. 1. This figure shows how the three methods described above are applied either in combination or singly to resolve the receiver bias. The first step in this process is to filter out data with elevation angles of less than 30° in order to separate out mapping function effects from the calculation of receiver bias. This is done because scalloping can be caused by both the receiver bias and a faulty mapping function. Above 30° elevation angle, all the mapping functions are very similar, and yet at 30° the slant delay is still almost twice the zenith delay at zenith. This leaves enough elevation angle effect to separate out the receiver bias.

Once the data with elevation angles greater than 30° has been collected, groups of sites are created by starting with a randomly selected seed site. Next all remaining available receiver sites are searched to find the receiver site in the closest proximity to any of the group members. If this identified site is within a 400 km horizontal distance, it is added to the group. The 400 km horizontal distance was chosen in order to ensure that within any group there would be a large number of coincident TEC measurements (defined as TEC estimates from different receivers that are separated by not more than 50 km in the horizontal location at the pierce point height of 450 km). This procedure is repeated until either there are no remaining sites within 400 km of any group member, or the group reaches a maximum number of 100 sites.

Once this step is complete, the method for determining the differential bias is dependent on the number of sites in the group. If the group consists of three or more sites, the differential biases are found using the least squares method which outputs relative, not absolute, biases. To set the level of the absolute bias, we could simply use the minimum scallop receiver bias for a single receiver. However, the minimum scallop technique has a certain amount of random uncertainty embedded in it. To reduce this uncertainty, we determine the minimum scallop receiver bias for all of the receivers in the group. We then find the average difference between these values and those computed by the least squares technique. In this way, the error in the absolute value of the receiver bias in the group is reduced by a factor of the square root of the number of receivers. Processing data from 1,000 stations takes approximately 12 h to run on a single computer with a Pentium 4 class CPU clock.

If the group contains fewer than three sites, the differential bias is found using the minimum scalloping technique. First, the zero TEC bias is computed and used as the initial guess. Next for a range of biases about the initial guess, a histogram of average TEC values versus elevation angle bin is constructed for data in a 4 h window centered on 2 a.m. local (solar) time. The slope of this histogram is calculated. If the minimum slope is at the edge of the range of biases, the process is assumed to have failed and the process is repeated with the histogram constructed for data in a 4 h window centered on solar noon. If the process fails a second time, it is repeated again with larger bias limits. In general, this process succeeds approximately 95% of the time.

The zero TEC method is employed in two cases. This method is used in the 5% of the cases where the minimum scalloping technique fails and it is automatically used for receivers located at latitudes above 65° latitude (or below − 65° latitude). The reason for this latitude criterion is illustrated in Fig. 3. Here, one can observe the highly variable TEC data from a receiver located near the South Pole, at the latitude of − 89.9978°. These fluctuations are typical of high latitude locations, and are larger in magnitude than the scalloping effect. Because of this, the minimum scalloping technique fails to work for high latitude data. The zero TEC method is a reasonable technique to apply because the overall level of TEC is less in the polar and sub-auroral regions than it is in the mid-latitude and equatorial regions (Jursa 1985).

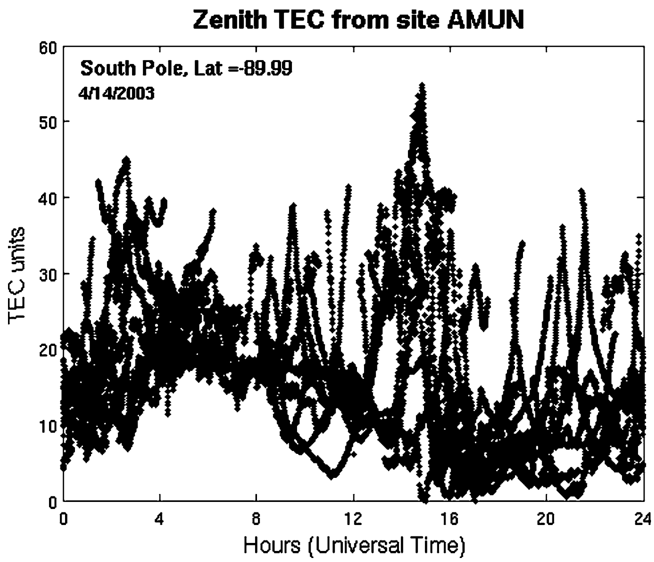

Fig. 3 Illustration of polar data where zero TEC method is used for determining the receiver bias

Removal of outliers

One of the important issues in processing multiple sites of GPS data is developing an algorithm which can catch outliers such as the one shown in Fig. 4. Typically when processing 2,000 receiver sites, 10–20 of the receivers will have data that looks like that shown in Fig. 4. In this case, a single receiver will observe TEC values from a single satellite that differ by a considerable amount, frequently many hundreds of TECU, from the TEC values observed by all other satellites in view. Because of the size of the differences observed, and the fact that these differences are observed over an entire satellite pass, this does not appear to be a physical phenomenon. To verify that this was not an issue with the MAPGPS code, we compared MAPGPS TEC measurements with those output by the University of Texas Applied Research Laboratory's (UTARL) code for a day when this type of phenomenon was observed (G. Bust, private communication). The data compared were from the AUCK site, day 324, year 2003. They observed the same phenomenon. They did note that the satellite data in question was associated with a lower SNR. It is assumed that this type of outlier is due to some issue in the firmware of the receiver. This possibility was suggested by R. Snow (private communication).

To identify this type of outlier, MAPGPS uses an algorithm to look at the TEC distribution of each receiver for each instance in time. If a single measurement of the TEC is 40 TECU above or below all of the others for that instance in time, a flag is set. Then, if in any given hour, over 10% of the data falls into this category, the criterion is considered met, and

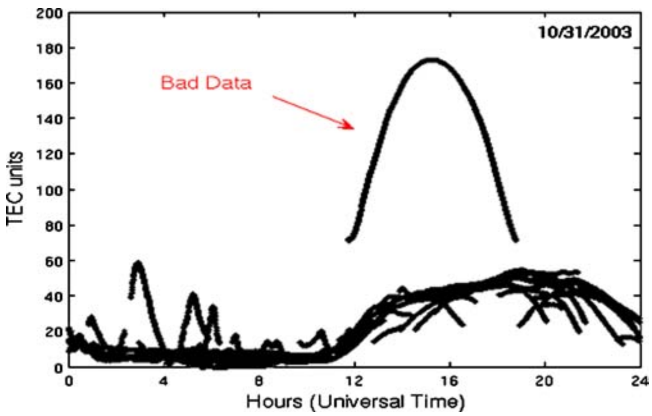

Fig. 4 Illustration of bad data for a single satellite

the TEC data from the entire pass of the anomalous satellite are removed.

One of the issues with this process is that a reasonable receiver bias needs to have been applied to the data in order to reliably detect the outliers. In MAPGPS, once the outliers have been detected and removed from the data, all receiver biases are recalculated for the group in which the outliers have been removed.

Comparison of JPL and MAPGPS receiver biases

To evaluate the JPL and MAPGPS processes, JPL (A. Komjathy, private communication) provided us with 150 receiver biases for 2 days. When we compared the JPL biases to those estimated by MAPGPS, we found that the biases that used the Zero TEC method alone had a median absolute difference of 5.0 TECU and a standard deviation of 6.8 TECU. The biases that used the scallop technique alone had a median absolute difference of 5.0 TEC and a standard deviation of 5.4 TECU. Finally, the biases that were determined using the least squares technique had a median standard difference of 2.7 TECU and a standard deviation of 2.5 TECU.

The least squares technique is used to estimate the receiver biases in regions where a large number of receivers are closely spaced. It is not surprising therefore that the differences between the MAPGPS and JPL techniques are smallest in regions, such as the continental US or Europe, where this condition is met. The differences between the MAPGPS and JPL techniques are largest in regions where the GPS receivers are relatively isolated, such as South America, Africa, Antarctica, and the Arctic.

To summarize this comparison, since the standard deviation of the distribution of receiver biases is 52 TECU, the two processes, JPL and MAPGPS, disagree only to the 10% level. The JPL receiver biases are more consistent than the MAPGPS receiver biases day-to-day. However, our noise figure of merit is increased if we replace our receiver biases with those of JPL.

A possible test, suggested by R.B. Langley (private communication) would be to determine coordinates of well-positioned receivers using TEC values calculated with both the MAPGPS and JPL receiver biases. The estimated coordinates could be compared to the published coordinates. The TEC values obtained using the more correct set of biases should produce receiver coordinates closer to the truth.

Temperature dependence in receiver biases

A potential systematic error source arises from the omission in either algorithm of the possibility of temperature changes over the course of the measurement. Parts of the GPS system that could be temperature dependent include the pre-amplifier, located within the GPS antenna, and the cables used to connect the antenna to the receiver. This section of the paper addresses this issue.

Figure 5 shows an example of an observed diurnal difference between TEC measurements collected from three closely spaced receivers (MHR0, WES2, WFRD). These measurements were collected during an experiment conducted as part of the 1995 Westford Water Vapor Experiment (Coster et al. 1996; Niell et al. 2001). All of these measurements were made with A.O.A. Turbo Rogue GPS receivers equipped with Dorne-Margolin choke-ring antennas. The receivers were located within 1 km of each other on the MIT Haystack Observatory site near Westford, MA. The MHRO antenna was located on a pole on the roof of the Millstone Radar building, the WES2 antenna was (and is) located on a 10 m tower behind the Westford Antenna, and the

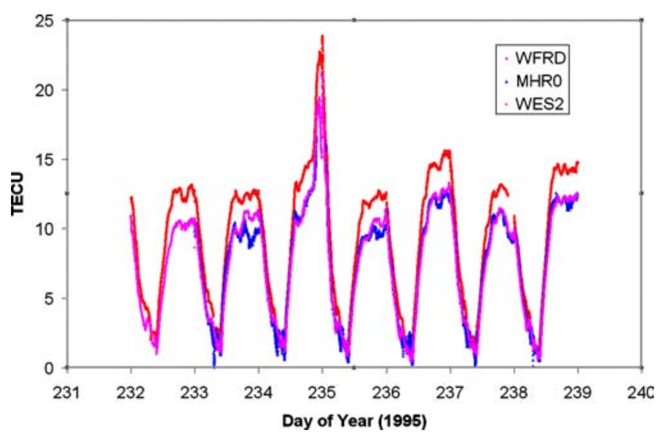

Fig. 5 Zenith TEC estimates measured by three closely spaced GPS receiver (WFRD, MHR0, and WES2). The time axis starts on 19 August 1995 (day 231) and ends on 28 August 1995 (day 240)

WFRD antenna was located on a ground mount covered by a plexiglass dome in the field next to the Westford antenna.

Figure 5 shows the estimated zenith TEC from GPS receivers at the MHRO (blue), WES2 (magenta), and WFRD (red) sites. This estimate is formed by averaging the line of sight TEC observations converted to zenith from all satellites in view. A single receiver bias for each day was estimated for each receiver. On all days of the experiment, the WFRD receiver measured approximately 3 TECU more than the WES2 and MHR0 receivers during the daytime starting around 14:00–15:00 UT. The minimum difference in the TEC between these sites was measured at 3:00–4:00 UT. Although the site locations were close, the field of view was not the same at the different sites, and this can possibly account for some of the observed difference in the diurnal measurement of TEC. A more likely explanation of the different TEC measurements is that the receiver bias of at least one of the receivers changed as a function of local temperature. During this experiment, the cables used to connect the receivers to the antennas at WES2 and WFRD were not the recommended low-loss cables and, in particular, the cable to the WFRD antenna lay on the ground and partially traversed a road. The plexiglass dome covering the WFRD antenna also ensured that this antenna endured a substantial increase in its temperature over that of the WES2 and MHR0 antennas during the day. This observation, in our opinion, demonstrates a potentially significant source of systematic error in GPS TEC analysis which should be further investigated by the larger GPS community.

Final TEC product from MAPGPS

The final TEC product from MAPGPS is output in a user-specified grid of degrees and time. The standard MAPGPS grid size is 1° by 1° by 5 min. For each bin in the grid, MAPGPS selects the median of all measurements within it to be the estimated value for that bin. Separately, for each receiver, files are produced that contain both the zenith TEC values and their associated pierce point locations, the value of the mapping function used, and the line of sight TEC values and their azimuth and elevation angles. This data is provided for every processed observation in the original RINEX file, although these files are not normally archived. One last point of note is that many of the sites now report data at the 1 Hz rate. Processing this amount of data requires a considerable amount of computation time and archival space. Because of this, MAPGPS offers the option of decimating the original data in time. Typically, MAPGPS decimates the original data stream to a final 0.05 Hz rate.

Madrigal

Madrigal is an open source, Web-based, distributed database system which provides the means for organizing, distributing, and searching a variety of scientific data products from a wide range of instrumentation. Originally, Madrigal stood for Millstone Analysis and Data Reduction Interactive Graphical Analysis Language. However, Madrigal is now officially just the name of an open source database project.

The Madrigal database has been developed at MIT Haystack Observatory primarily for the purpose of managing incoherent scatter radar data and has evolved to include a wide range of data, model, and derived products. Incorporating other types of data into Madrigal is relatively easy and usually involves modification of the data generating software to use compatible output formats and Web-based hyperlinks. Madrigal supports sophisticated searching and enables the real-time delivery of data in a variety of standardized formats including that used by the National Center for Atmospheric Research (NCAR) Coupling, Energetics, and Dynamics of Atmospheric Regions (CEDAR) data system, (Sica et al. 1988). Development of Madrigal is ongoing and planned upgrades include improved online visualization capabilities as well as improvements in the Web-based interfaces.

In June 2005, GPS TEC data was incorporated into Madrigal, and can be accessed through the Web site http://www.haystack.mit.edu/madrigal. A simple Madrigal data access function has recently been added, and the worldwide GPS data is available as one of the many supported instruments. Approximately 250 days have been processed at this time. The data is provided as estimates of TEC in 1° by 1° bins every 5 min distributed over locations where GPS data is available. TEC maps representing an integration of TEC data every 20 min throughout the day are provided. An example is shown in Fig. 6.

The Madrigal database has been an invaluable tool for many long-term scientific studies using incoherent scatter data (Lei et al. 2004, 2005; Zhang et al. 2004, 2005). We anticipate that the availability of global TEC data through Madrigal will prove an equally significant resource for future scientific studies.

Summary

The automated processing of GPS data from the global network of receivers requires attention to a multitude of details and intensive processing. In this paper, we have outlined the procedures that are used by MAPGPS to process this data. We have also described where and how to access the 1° by 1° TEC data produced by MAPGPS. At MIT Haystack, MAPGPS

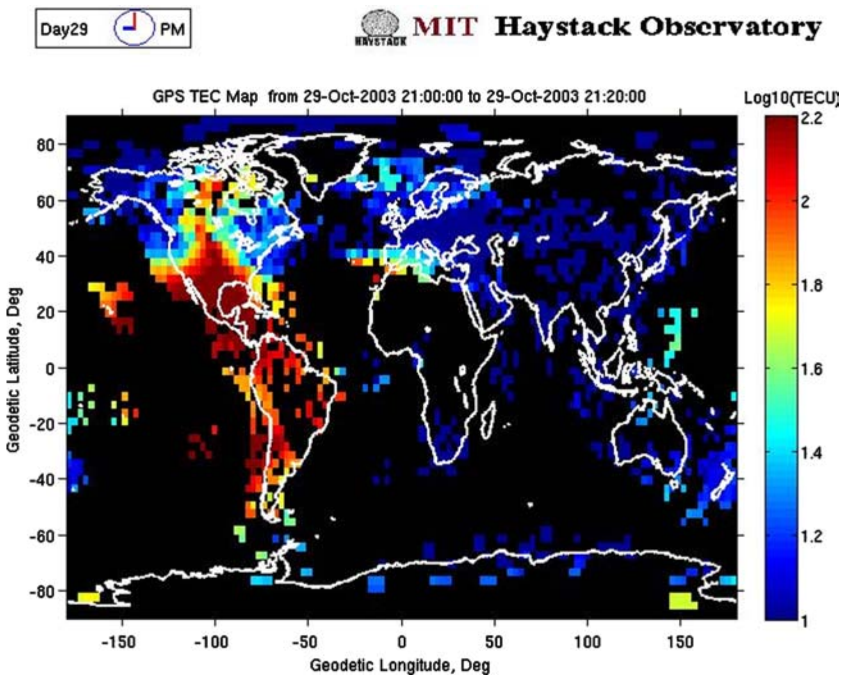

Fig. 6 Example of TEC map available on Madrigal. The map represents an integration of all of the TEC data available in the interval from 21:00:00 to 21:20:00 UT

continues to evolve as we refine and improve our algorithms and our data delivery.

The advantage to our process is that it is strictly data-driven, with no underlying models that smooth out real gradients in the TEC. The disadvantage is that by using all available GPS data one introduces some uncertainty to the estimate of TEC. At this time, we do not provide estimates of the uncertainty in either our receiver bias estimation or our TEC estimation.

Our future plans for MAPGPS include incorporating the uncertainty information into our estimation procedure and examining mapping function issues in greater detail. We also plan to test the idea of solving for the receiver biases as a function of time of day to account for temperature dependencies. In the near term, we intend to incorporate historical TEC data into the Madrigal database for general use by the atmospheric science community. A large amount of science has already been accomplished using the small amount of existing TEC data (Foster et al. 2002, 2004, 2005a, b; Nicolls et al. 2004; Coster et al. 2006). We expect even more discoveries to be made using this new, complete database of TEC data.

Acknowledgments The authors would like to thank Dr. Marlene Colerico for her help with the figures and other members of the MIT Haystack Observatory staff for their support. The authors would also like to thank the reviewers for their careful readings. Their suggestions significantly improved the content of this paper.

References

Blewitt G (1990) An automatic editing algorithm for GPS data. Geophys Res Lett 17(3):199–202

Coster A, Skone S, Taylor B, Colerico M (2006) Analysis of mid-latitude space weather events and their user impacts. In: Proceedings of ION NTM 2006. Monterey, CA, pp 1028–1035

Coster AJ, Niell AE, Solheim FS, Mendes VB, Toor PC, Buchmann KP, Upham CA (1996) Measurements of precipitable water vapor by GPS, radiosondes, and a microwave water vapor radiometer. In: Proceedings of ION GPS-96, Kansas City, MO, 17–20 September 1996, pp 625–634

Coster AJ, Foster JC, Erickson PJ, Rich FJ (2001) Regional GPS mapping of storm enhanced density during the 15–16 July 2000 geomagnetic storm. In: Proceedings of ION GPS 2001, 11–14 September 2001, Salt Lake City, Utah, pp 2531–2539

Feltens J, Schaer S (1998) IGS products for the ionosphere, In: Proceedings of IGS 1998 analysis center workshop, ESOC, Darmstadt, Germany, February 9–11, pp 225–232

Foster JC, Erickson PJ, Coster AJ, Goldstein J, Rich FJ (2002) Ionospheric signatures of plasmaspheric tails. Geophys Res Lett 29(13). DOI 10.1029/2002GL015067

Foster JC, Coster AJ, Erickson PJ, Rich FJ, Sandel BR (2004), Stormtime observations of the flux of plasmaspheric ions to the dayside cusp/magnetopause. Geophys Res Lett 31. DOI 1029/2004GL020082

Foster JC, Coster AJ, Erickson PJ, Rideout W, Rich FJ, Immel TJ, Sandel BR (2005a) Redistribution of the stormtime ionosphere and the formation of a plasmaspheric bulge, Inner magnetosphere interactions: new perspectives from imaging. Geophys Monograph Ser 159. DOI 10.1029/159GM21

Foster JC, Coster AJ, Erickson PJ, Holt JM, Lind FD, Rideout W, McCready M, van Eyken A, Barnes RJ, Greenwald RA, Rich FJ (2005b), Multiradar observations of the polar tongue of ionization, J Geophys Res 110. DOI 10.1029/2004JA010928

Fuller-Rowell T (2005) USTEC: a new product from the space environment center characterizing the ionospheric total electron content. GPS Solutions 9(3):236–239. DOI 10.1007/s10291-005-0005-5

Gaposchkin EM, Coster AJ (1993) GPS L1–L2 bias determination, Technical Report 971, MIT Lincoln Laboratory, 12 January 1993

Hernandez-Pajares M, Juan JM, Sanz J (1999) New approaches in global ionospheric determination using ground GPS data. J Atmos Sol Terr Phy 61:1237–1247

Jursa A (ed) (1985) Handbook of geophysics and the space environment, Air Force Geophysics Laboratory, Air Force Systems Command, U.S. Air Force

Komjathy A (1997) Global ionospheric total electron content mapping using the global positioning system. Ph.D. dissertation, Department of Geodesy and Geomatics Engineering Technical Report No. 188, University of New Brunswick, Fredericton, New Brunswick, Canada, 248 pp

Komjathy A, Langley RB (1996) The effect of shell height on high precision ionospheric modelling using GPS. In: Proceedings of the international GPS service for geodynamics (IGS) workshop in Silver Spring, MD, 19–21 March 1996, pp 193–203

Komjathy A, Sparks L, Wilson BD, Mannucci AJ (2005) Automated daily processing of more than 1,000 ground-based GPS receivers for studying intense ionospheric storms. Radio Sci 40, RS6006. DOI 10.1029/2005RS003279

Lei J, Liu L, Wan W, Zhang S-R, Holt JM (2004) A statistical study of ionospheric profile parameters derived from Millstone Hill incoherent scatter radar measurements. Geophys Res Lett 31(14), L14804. DOI 10.1029/2004GL020578

Lei J, Liu L, Wan W, Zhang S-R (2005) Variations of eletron density based on long-term incoherent scatter radar and ionosonde measurements over Millstone Hill. Radio Sci 40, RS2008. DOI 10.1029/2004RS003106

Mannucci A, Wilson B, Edwards C (1993) A new method for monitoring the earth's ionospheric total electron content using the GPS global network. In: Proceedings of ION GPS-93, the 6th international technical meeting of the satellite division of The Institute of Navigation, Salt Lake City, UT, 22–24 September 1993, pp 1323–1332

Mannucci AJ, Wilson BD, Yuan DN, Ho CH, Lindqwister UJ, Runge TF (1998) A global mapping technique for GPS-derived ionospheric total electron content measurements. Radio Sci 33(3):565–583

Nicolls MJ, Kelly MC, Coster AJ, Gonzalez SA, Makela JJ (2004) Imaging the structure of a large-scale TID using ISR and TEC Data. Geophys Res Lett 31, L09812. DOI 10.1029/2004GC 019797

Niell AE, Coster AJ, Solheim FS, Mendes VB, Toor PC, Langley RB, Upham CA (2001) Comparison of measurements of atmospheric wet delay by radiosonde, water vapor radiometer, GPS, and VLBI. J Atmos Ocean Tech 18:830–850

Renfro B, Harris RB, Tolman BW, Gaussiran T, Munton D, Little J, Mach R, Nelsen S (2005) The open source GPS toolkit: a review of the first year. In: Proceedings of ION GNSS 2005, the 18th international technical meeting of the satellite division of The Institute of Navigation, Long Beach, CA, 13–16 September 2005, pp 543–551

Sardon E, Rius A, Zarraoa N (1994) Estimation of the transmitter and receiver differential biases and the ionospheric total electron content from global positioning system observations. Radio Science 29(3):577–586

Sica RJ, Richmond AD, Emery BA, Chakrabarti S, Wickwar VB (1988) The CEDAR data base. Eos Trans AGU 69(3):35

Wilson BD, Yinger CH, Feess WA, Shank C (1999) New and improved—the broadcast interfrequency biases. GPS World 10(9):56–66

Zhang S-R, Holt JM, Zalucha AM, Amory-Mazaudier C (2004) Mid-latitude ionospheric plasma temperature climatology and empirical model based on Saint Santin incoherent scatter radar data from 1966–1987. J Geophys Res 109, A11311. DOI 10.1029/2004JA010709

Zhang S-R, Holt JM, van Eyken AP, McCready M, Amory-Mazaudier C, Fukao S, Sulzer M (2005) Ionospheric local model and climatology from long-term databases of multiple incoherent scatter radars. Geophys Res Lett 32, L20102. DOI 10.1029/2005GL023603